Proceedings of the
44th IEEE Conference on Decision and Control, and
the European Control Conference 2005
Seville, Spain, December 12-15, 2005

ThC16.2

Time-energy optimal control of hyper-actuated mechanical systems with geometric path constraints

J.B. Aldrich and R.E. Skelton[*][†]

Abstract

For a general class of Hyper-Actuated Mechanical Systems (HAMS) that is generalized to include robotic manipulators and tendon-driven tensegrity structures, this paper determines the tendon force inputs from a set of admissible, non-saturating inputs, that will move the rigid-body system from point A to point B along a prescribed path with minimum time and control energy. The approach herein utilizes the existence conditions and solution of a linear algebra problem that describes how the set of admissible tendon forces is mapped onto the set of path-dependent torques. Since this mapping is not one-to-one, free parameters in the control law always exist. This paper determines the best time-invariant free parameters. This yields a novel control law for HAMS that tracks the center of the admissible set and reduces the number of states in the optimal control problem to two. The prevalence of HAMS in nature is discussed. Numerical examples illustrate the method and demonstrate tensegrity's superior maneuvering and saturation avoidance capabilities.

1. Introduction

An important consideration in the robotic automation of dull, difficult or dangerous tasks is optimal control. This is especially true when a specific task or desired maneuver has been identified either by sensing/processing capabilities of the robot (on-line) or its operator (off-line). In either case, it is natural to ask how fast can this be done, and how much control energy is required. The answer to this question depends on the inertial dynamics of the robot, its actuator limitations and the desired course of reconfiguration. This is essentially the time-energy optimal control problem that has been discussed in many texts on optimal control. For Joint-Actuated Mechanical Systems (JAMS),

Figure 1. (Left) The musculoskeletal model of a cat's hindlimb consists of 8 actuators (muscles) and 3 joints. The hindlimb is an example from nature of a hyper-actuated mechanical system (HAMS). (Right) Typical joint-actuated mechanical system (JAMS). An obvious advantage of HAMS over JAMS is force-leverage, so why not mimic nature?

this problem has been studied extensively in [3, 7, 5]. All these studies were limited to collocated actuation systems where the number of actuators must be the same as the number of degrees-of-freedom. This paper extends these results by allowing more actuators than degrees of freedom. This extension is not trivial as the actuation redundancy must be considered within the optimal control problem. If additional states are included to account for this particular redundancy, the problem becomes complicated by the so-called curse of dimensionality often attributed to problems in optimal control [4]. In order to circumvent this problem, this paper introduces a control law with the property that the actuation redundancy is used to track the center of the admissible set of control inputs. This proves to be a nonrestrictive feature since the proposed control law has a natural saturation-avoidance property. By imposing this control law, this paper solves the time-energy optimal control problem for the hyper-actuated mechanical systems (HAMS) case using the classical Hamiltonian approach.

Control theorists and engineers often focus great attention on controllability to determine the *minimal* number of actuators required to control a system. Nature does the opposite. A Grasshopper has 6 degrees of freedom, but uses 270 different control muscles to be more energy efficient and more robust to uncertainty in load directions. This point is illustrated also in the cat's hindlimb in figure (1). Hence, HAMS is naturally selected in biological systems.

---
[*]J.B. Aldrich is with the Caltech/JPL Postdoctoral Scholars Program, Jet Propulsion Laboratory, Pasadena, CA 91109, USA, `jaldrich@jpl.nasa.gov`

[†]Professor R.E. Skelton is with the Department of Mechanical and Aerospace Engineering, at the University of California, San Diego, La Jolla, CA 92093, USA, `bobskelton@ucsd.edu`

Arguably, the most general framework for studying both HAMS and JAMS alike is the tensegrity structure paradigm [6, 2], where there is an abundance of tendons and/or joint motors that can be controlled. Tensegrity structures become tensegrity robots once adequate tendon actuation technology is implemented. An example of a planar tensegrity robot is illustrated in figure (2) and candidate tendon actuation technology is illustrated in figure (3). It is natural to ask, "Can tensegrity compete with state-of-the-art robotics?" As a case in point, the classical Stewart-bridge robot in figure (4) is not HAMS and is not capable of the same workspace as its tensegrity counterpart in figure (3). Another disadvantage of the Stewart-bridge is the edge-actuators are bulky and cannot change their contour when the robot is in contact with its environment. On the other hand, tensegrity is malleable, and can change its crosection/volume/area to accomplish unusual tasks that are not allowed in the conventional robot.
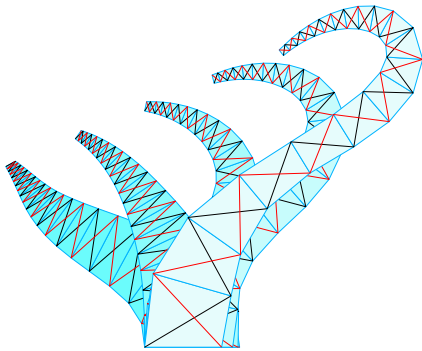
Figure 2. A maneuver sequence for a planar tensegrity robotic manipulator with fixed-length rigid-bars (cross-diagonal lines) and adjustable-length control tendons (all other lines). Notice that the boundary of the robot consists exclusively of flexible tendons. Consequently, the robot's overall shape and exterior surface are malleable and capable of being controlled independently.

These illustrations and the work herein suggest that tensegrity concepts will revolutionize the manner in which tendon-driven systems are designed, controlled and utilized. We believe this will become especially true in environments where agile maneuvering and delicate object handling require a "soft" touch.

In the sections that follow, we address the following questions: What is HAMS in terms of relevant equations and conditions? Given a set of admissible tendon forces how should the control law be designed? How can the expended energy and acquisition time be minimized as the robot moves along a prescribed path?
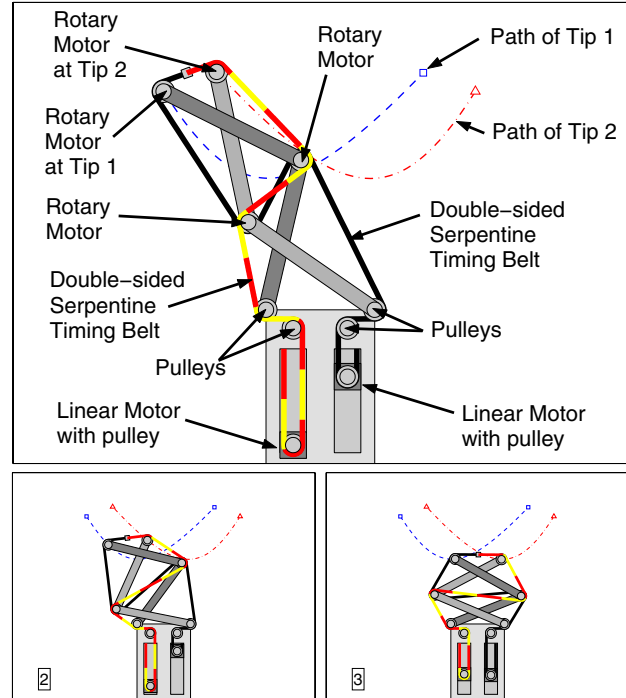
Figure 3. Two stage tensegrity robot. A single serpentine timing belt is shown driving the entire 4 degree-of-freedom robot along two independently-defined tip-paths. Simple geometric relationships are used to command the relative angles for the rotary motors and the vertical position of the linear motors such that the inextensible serpentine timing belt never goes slack at any point within the tendon network.

2. Hyper-Actuated Mechanical Systems

Given a rigid-body mechanical system with degrees of freedom $q \in \mathbb{R}^n$ governed by the equations of motion

$$M(q)\ddot{q} + V(q,\dot{q})\dot{q} + g(q) = \tau \tag{1}$$

the system is said to be a *hyper-actuated mechanical system (HAMS)* if the applied torques $\tau \in \mathbb{R}^n$ are implemented by actuator forces $t \in \mathbb{R}^m$ according to

$$\tau = G(q)t \tag{2}$$

and the following condition holds

$$G \in \mathbb{R}^{n \times m}, \quad m > n, \quad \text{rank}(G) = n \tag{3}$$

Since actuators are force-limited, the actuator force vector, $t \in \mathbb{R}^m$, must belong to an admissible set defined by

$$\mathscr{A} := \{t \in \mathbb{R}^m : t_{MIN_i} \leq t_i \leq t_{MAX_i}\} \tag{4}$$
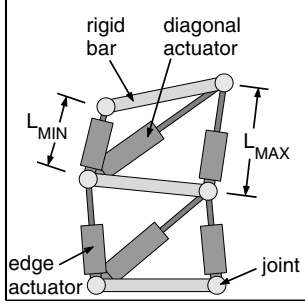
Figure 4. A two-stage Stewart-Bridge robot. (non-HAMS) Four edge-actuators and two diagonal-actuators are connected between three rigid bars as shown. The maximum stroke L_{MAX} and minimum stroke L_{MIN} for an edge-actuator are also indicated above. For a fixed bottom bar, the system has six degrees-of-freedom. Its workspace is generally much smaller than in figure (3) due to the inherent actuator-stroke limitations of bi-directional actuation systems.

where t_i is the tension of the ith actuator, t_{MIN_i} is the minimum allowable tension for the ith actuator, and t_{MAX_i} is the maximum allowable tension for the ith actuator.

In order to avoid loss of kinematic control, the paper assumes the robot's position $r = r(q)$ does not pass through points where the Jacobian matrix $J(q) = \frac{dr}{dq} \in \mathbb{R}^{n \times n}$ becomes singular. This condition is combined with (3) and (4) to define the HAMS workspace $\mathscr{W}$ as

$$\mathscr{W} := \left\{ y \in \mathbb{R}^n \left| \begin{array}{c} \exists q \in \mathbb{R}^n \text{ s.t. } y = r(q), \\ J(q) \text{ invertible}, \\ G(q) \text{ full row rank}, \\ Gt = 0 \text{ for some } t \in \mathscr{A} \end{array} \right. \right\} \quad (5)$$

3. Center-tracking control law

By virtue of condition (3), there exists an infinite number of solutions to (2). This paper focuses on one particular solution of (2) given by

$$t = G^+ \tau + G^\perp c \quad (6)$$

where τ is defined in (1),

$$G^+ = G^T W, \quad G^\perp = [I - G^T W G], \quad W = (GG^T)^{-1} \quad (7)$$

and c defines the center of the admissible set as

$$c := \text{center}(\mathscr{A}) = (t_{MIN} + t_{MAX})/2 \quad (8)$$

Equation (6) will be referred to in this paper as the center-tracking control law (CTCL) because it is the unique solution to the following optimization problem.

$$\min_{Gt=\tau} \|t - c\|^2$$

Remark 1. The CTCL is effective at keeping the control tendons from breaking or going slack (saturation avoidance, [2]), because it chooses t as close as possible to the center of the admissible set, c, while satisfying the dynamic constraint $Gt = \tau$.

Remark 2. Alternatively, the CTCL can be viewed as the sum of static and dynamic forces, $t = t_{stat} + t_{dyn}$, where

$$\begin{aligned} t_{dyn} &= \arg \min_{Gt=\tau} \|t\|^2 = G^+ \tau \\ t_{stat} &= \arg \min_{Gt=0} \|t - c\|^2 = G^\perp c \end{aligned}$$

That is, t_{dyn} contains the smallest (2-norm) actuator forces that can sustain loading τ. And t_{stat} is as close as possible to c subject to the static equilibrium constraint $Gt = 0$.

In practice, t_{stat} can be sustained with zero expended control energy by using non-backdriveable gears between the tendons and the motors. Hence, the expended control energy is the dynamic, not static, force density defined as

$$\begin{aligned} \text{Control energy:} \quad \mathscr{U} &= t_{dyn}^T t_{dyn} \\ &= \tau^T (GG^T)^{-1} \tau \quad (9) \\ &= \|t - t_{stat}\|^2 \end{aligned}$$

It is worthwhile to note that the last expression above can be rewritten as $\mathscr{U} = \|t - t_{stat}(q)\|^2$, where $t_{stat}(q)$ is a quasi-static equilibrium force trajectory for slowly varying q. With this is mind, $\mathscr{U}$ is a measure of the system's deviation from the static equilibrium manifold.

4. Time-energy optimal control along a path

In this section, a time-energy optimal control problem is solved for the case that the robot's position $r = r(q)$ is constrained to move on the following path constraint

$$r(q) = \tilde{r}(s) \in \mathscr{W}, \quad \forall s \in [s_o, s_f] \subset \mathbb{R} \quad (10)$$

where $\tilde{r}$ is a user-defined polynomial function of s [2].

The time/energy cost function in (11) consists of an ε-weighted combination of the acquisition time T and the expended control energy $\mathscr{U}$.

Problem statement. Determine the non-saturating actuator forces $t \in \mathscr{A} \subset \mathbb{R}^m$ governed by the center-tracking control law that will move the plant from point-to-point along

a prescribed path with minimal time/energy cost. That is,

$$\min_{t\in\Re^m}\int_0^T 1+\varepsilon^2\|t-t_{stat}\|^2\,d\hat{t} \quad\bigg|\quad \text{cost}$$

s.t.

$t\in\mathscr{A}$	actuator admissibility
$t_{stat}=G^\perp(q)c$	static equilibrium
$t=t_{stat}+G^+(q)\tau$	control law
$M(q)\ddot{q}+V(q,\dot{q})\dot{q}+g(q)=\tau$	dynamics
$r(q)=\tilde{r}(s)$	path constraint
$q(0)=q_o,\ \dot{q}(0)=0$	initial conditions
$q(T)=q_T,\ \dot{q}(T)=0$	terminal conditions

(11)

where T denotes the unspecified terminal time, $\hat{t}$ denotes time. (Recall, t denotes actuator forces.) To solve this problem, the cost and constraints will be defined in terms of the path variables,

$$x=[\ x_1\quad x_2\ ]^T\equiv[\ s\quad \dot{s}\ ]^T,\qquad \ddot{s}=u\in\mathbb{R}$$

The path constraint $r(q)=\tilde{r}(s)$ can be used to rewrite the system dynamics (1) in terms of the path variables as follows. (See [3, 7, 2] for details of this transformation.)

$$\tau=d(x_1)u+x_2^2 b(x_1) \tag{12}$$

For $R=\mathrm{diag}\left[(t_{MAX}-t_{MIN})/2\right]$, it was shown in [2] that

$$t\in\mathscr{A}\quad\Leftrightarrow\quad \|R^{-1}(t-c)\|_\infty\le 1 \tag{13}$$

Hence, (12) can be substituted into the CTCL control law $t=G^+\tau+G^\perp c$, followed by substitution into the admissibility constraint (13), to get $\|w(x_1)u+y(x)\|_\infty\le 1$ where

$$w=R^{-1}G^+d \qquad y=R^{-1}(G^+bx_2^2-G^{+T}c) \tag{14}$$

Equivalently, $-1\le y_i(x)+uw_i(x_1)\le 1$ for $i=1$ to m. Further rearrangement yields the following constraint on u.

$$u_{min}(x)\le u\le u_{max}(x) \tag{15}$$
$$u_{min}(x)=\max\left\{\Phi_i^{LO}(x):i=1,2,\ldots,m\right\}$$
$$u_{max}(x)=\min\left\{\Phi_i^{HI}(x):i=1,2,\ldots,m\right\}$$

where the "influence functions", namely Φ_i^{LO} and Φ_i^{HI}, are

$$\Phi_i^{LO}=-1/|w_i|\ -\ y_i/w_i \tag{16}$$
$$\Phi_i^{HI}=+1/|w_i|\ -\ y_i/w_i$$

Hence, the state-dependent control constraint is

$$g(x,u)=[\ g_1\quad g_2\ ]^T\le 0$$
$$g_1=u-u_{max}(x),\quad g_2=u_{min}(x)-u$$

and the state-dependent existence condition for $u\in\mathbb{R}$ satisfying (15) is given by

$$h(x)=u_{min}(x)-u_{max}(x)\le 0 \tag{17}$$

The Lagrangian $L=1+\varepsilon^2\|t-t_{stat}\|^2$ becomes

$$L(x,u)=1+\varepsilon^2\tau^T W\tau \tag{18}$$

where $\tau=\tau(x,u)$ is given explicitly in (12) and $W=W(x_1)$ is given in (7). In summary, assuming (17) holds, problem (11) is equivalent to problem (19) below.

$$\min_{u\in\Re}\int_0^T L(x,u)\,d\hat{t}$$

s.t.

$\dot{x}=f(x,u)=[\ x_2\quad u\ ]^T$	path dynamics, (a)
$x_1(0)=s_o,\ x_2(0)=0$	initial conditions, (b)
$x_1(T)=s_f,\ x_2(T)=0$	terminal conditions, (c)
$g(x,u)\le 0$	saturation constraint, (d)

(19)

The Hamiltonian $H=L(x,u)+\lambda^T f(x,u)+\mu^T g(x,u)$ for problem (19) becomes

$$H=1+\lambda_1 x_2+\lambda_2 u+\mu^T g+\varepsilon^2\tau^T W\tau \tag{20}$$

In order to solve problem (19), the following necessary conditions [4] must hold.

Necessary conditions for the optimal control. There must exist nontrivial solutions $\lambda^*(\hat{t})$ and $x^*(\hat{t})$ (where $\hat{t}$ denotes time) to the state and costate equations

$$\dot{\lambda}\ =\ -H_x^T=-L_x^T-f_x^T\lambda-g_x^T\mu \tag{21}$$
$$\dot{x}\ =\ f(x,u) \tag{22}$$

such that

$$H=0\quad\text{at}\quad\hat{t}=T \tag{23}$$
$$H_u=0\quad\text{for}\quad 0\le\hat{t}\le T \tag{24}$$
$$\mu_i\begin{cases}\ge 0,&g_i=0\\=0,&g_i<0\end{cases}\quad i=1,2. \tag{25}$$

and the following two-point boundary conditions

$$x_1(0)=s_o,\quad x_2(0)=0,\quad x_1(T)=s_f,\quad x_2(T)=0 \tag{26}$$

are satisfied.

Solution. If $\lambda^*(\hat{t})$ and $x^*(\hat{t})$ are computed such that (21), (22) (23), (24), (25) and (26) hold, then we can conclude that the necessary conditions of optimality for problem (19) are satisfied. This is our task. The following claim gives sufficient conditions for completing this task.

Theorem 1 *Suppose $\varepsilon>0$ and that the trajectories $\lambda^*(\hat{t}),x^*(\hat{t})\in\mathbb{R}^2$ for $\hat{t}\in[0,T]$ exist to solve the following system of ode's*

$$\dot{\lambda}_1\ =\ -\varepsilon^2\tau^T\left[2W(ud_{x_1}+x_2^2 b_{x_1})+W_{x_1}\tau\right]-\mu^T g_{x_1} \tag{27}$$
$$\dot{\lambda}_2\ =\ -\lambda_1-4\varepsilon^2 x_2 b^T W\tau-\mu^T g_{x_2} \tag{28}$$
$$\dot{x}_1\ =\ x_2 \tag{29}$$
$$\dot{x}_2\ =\ u \tag{30}$$

with initial conditions $\lambda_1(0) = \lambda_{01}$, $\lambda_2(0) = \lambda_{02}$, $x_1(0) = 0$ and $x_2(0) = 0$, where $u, \mu_1, \mu_2, \lambda_{02} \in \mathbb{R}$ are given below by (33, 35), and $\lambda_{01} \in \mathbb{R}$ is chosen such that the path velocity is zero at the end of the maneuver, i.e. $x_1(T) = s_f$, $x_2(T) = 0$. Then, the necessary conditions of optimality for problem (19) are satisfied provided the following additional conditions are also satisfied.

(i.) $h(x) \leq 0$ holds for all $x \in \{x^*(\hat{t}) : \hat{t} \in [0, T]\}$

(ii.) $W(x_1)$ is positive definite for all $x_1 \in [0, s_f] \subset \mathbb{R}$

Proof. The Hamiltonian is formed as in (20), and its gradient with respect to the state is substituted into (21) to yield the two first-order costate differential equations $\dot{\lambda}_1 = -H_{x_1}$ (27) and $\dot{\lambda}_2 = -H_{x_2}$ (28). Substituting the Hamiltonian gradient with respect to u into $H_u = 0$ (24) yields

$$\lambda_2 + \mu_1 - \mu_2 + 2\varepsilon^2(d^T W b)x_2^2 + 2\varepsilon^2(d^T W d)u = 0 \quad (31)$$

By hypothesis (*ii.*), W is positive definite ($W = [GG^T]^{-1}$ with G full row rank) which implies that the Hamiltonian is strictly convex provided $d \neq 0 \in \mathbb{R}^n$ (i.e. $H_{uu} = d^T W d > 0$). Suppose $d = 0 \in \mathbb{R}^n$, then $u = \infty$ is admissible. This is a contradiction, therefore $d \neq 0 \in \mathbb{R}^n$ and the Hamiltonian is strictly convex in u. Consequently, the optimal $u^* \in \mathbb{R}$ is uniquely defined by (31). That is, singular solutions for the control u does not exist.

In order to prevent u from violating its constraints $g(x, u) \leq 0$, the control $u \in \mathbb{R}$ and multipliers $\mu \in \mathbb{R}^2$ are determined by a "switching" function $\sigma : \mathbb{R}^3 \rightarrow \mathbb{R}$ given by

$$\sigma(x, \lambda_2) = \frac{-\lambda_2 - 2\varepsilon^2 d^T W b x_2^2}{2\varepsilon^2 d^T W d} \quad (32)$$

That is, the reader should verify that (31) and (25) are satisfied if

$$\{u, \mu_1, \mu_2\} = \begin{cases} \{u_{min}, & 0, & \mu_2^*\}, & \sigma \in (-\infty, u_{min}] \\ \{\sigma, & 0, & 0\}, & \sigma \in (u_{min}, u_{max}) \\ \{u_{max}, & \mu_1^*, & 0\}, & \sigma \in [u_{max}, \infty) \end{cases} \quad (33)$$

where

$$\mu_1^* = 2\varepsilon^2(\sigma - u_{max})d^T W d$$
$$\mu_2^* = 2\varepsilon^2(u_{min} - \sigma)d^T W d$$

It is also left as an exercise to the reader to show that the initial condition of the second costate $\lambda_2(0) \in \mathbb{R}$ is determined by the value of the following "decision" constant

$$\gamma = \frac{1}{\sqrt{\varepsilon^2 d^T(0)W(0)d(0)}} \quad (34)$$

That is, we can show that the optimality condition $H = 0$ at $\hat{t} = T$ (23) is satisfied if $\lambda_2(0) = \lambda_{02}$ where

$$\lambda_{02} = \begin{cases} -2\sqrt{\varepsilon^2 m_o}, & \gamma \in [0, u_{max}) \\ -1/u_{max}(0) - \varepsilon^2 m_o u_{max}(0), & \gamma \in [u_{max}, \infty) \end{cases} \quad (35)$$

where $m_o = d^T(0)W(0)d(0)$.

To see this is indeed the case, first observe that it suffices to show $H = 0$ at $\hat{t} = 0$ instead of showing $H = 0$ at $\hat{t} = T$ because H is necessarily constant (i.e. $\dot{H} = 0$ follows from $H_u = 0$, $\dot{\lambda} = -H_x^T$ and the fact that H is not an explicit function of time, $H_{\hat{t}} = 0$). Furthermore, because the robot is initially at rest $x_2(0) = 0$, $u \geq 0$ is necessary at time $\hat{t} = 0$ in order to avoid moving "backwards" along the path. Hence, only two cases are possible at time $\hat{t} = 0$: (a) $u = \sigma \in [0, u_{max})$ or (b) $u = u_{max}$. Substituting $x_2(0) = 0$ into H given by (20) and solving $H = 0$ for $\lambda_2(0)$ yields $u = \sigma = \gamma$ provided case (a) holds. Otherwise, case (b) follows by solving $H = 0$ with $u = u_{max}(0)$.

Finally, hypothesis (i.) must hold in order for there to exist an admissible control $u(\hat{t}) \in \mathscr{A}$ for all $\hat{t} \in [0, T]$. $\diamond$

Algorithm. Notice that there is only one missing initial condition, $\lambda_{01} \in \mathbb{R}$, which must be chosen such that the path velocity is zero at the end of the maneuver, i.e. $x_1(T) = s_f$, $x_2(T) = 0$. The correct λ_{01} can be determined by the following iterative search that ends once the terminal conditions are satisfied.

1. Compute $\lambda_{02} \in \mathbb{R}$ using (35).

2. Guess the first costate, $\lambda_{01} \in \mathbb{R}$.

3. Integrate the state and costate equations forward in time from their initial conditions (27 - 30). Continue numerical integration until the terminal condition $x_1(T) = s_f$ is reached.

4. If $x_2(T) \neq 0$, go to step 2 and repeat, else if $x_2(T) = 0$, then the algorithm has converged successfully to the candidate solutions $\lambda^*(\hat{t})$ and $x^*(\hat{t})$.

5. Using x^* and u^*, check condition (i.) in theorem (1). If this condition is not satisfied, then discard all output and quit. Otherwise, all conditions are satisfied and $(s(\hat{t}), \dot{s}(\hat{t})) = x^*(\hat{t})$ for $\hat{t} \in [0, T]$ is the optimal path trajectory for the time-energy optimal control problem.

This is a very simple algorithm compared to the typical dynamic programming case where $2n$ initial conditions must be determined for a mechanical system with n degrees of freedom.

4.1. Example and simulations.

In this section, the time-energy optimal control law is computed for a two stage planar rigid body robot driven by a tensegrity tendon network along a prescribed path. In figure (5) a sequence of the tensegrity robot moving along a user-defined path is shown. The robot considered here consists of six adjustable length tendons that are independently controllable and are responsible for moving the 4-link (2 serial chains each having two links per chain) rigid-body system along the path as shown. The first step in the time-
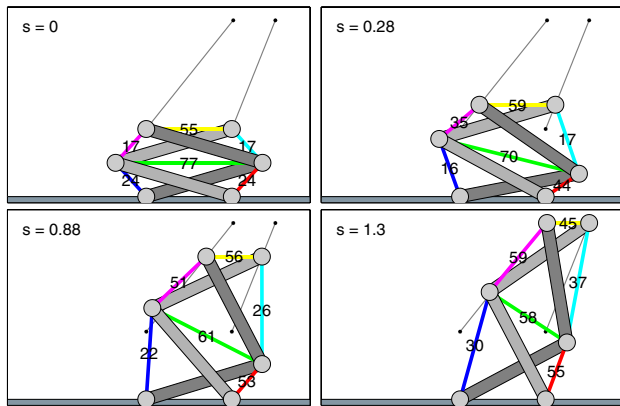
Figure 5. Tensegrity robot moving along specified path at various distances, s, along the path. Numbers on tendons indicate typical static equilibrium forces ($\tau = 0$) where the admissible set is $\mathscr{A} = \{t \in \mathfrak{R}^m : 0 \leq t_i \leq 100N\}$

energy optimal solution procedure is to guess the optimal value of the initial costate λ_{01} with hopes that the final configuration of the robot is the desired one and that the robot arrives at this final configuration with zero velocity. This is easier than it sounds. Use $\lambda_{01} = 0$ as a first guess. After the state/costate ODE is integrated from this initial condition, the integration routine is commanded to stop once the path velocity crosses zero from above. At this point only one of two outcomes is possible, the robot moved too far or too little along the path. To update λ_{01}, we observe that the total distance travelled along the designated path increases monotonically with our guess of λ_{01}. This property is illustrated in figure (6) where the time-trajectories of the the two states and two costates are illustrated for the robot maneuver illustrated in figure (5). Hence, when the robot comes to a halt at a position that overshoots (undershoots) its desired final destination, one should reduce (increase) the next guess for λ_{01}.

In figure (7), the path velocity x_2 function of time is pictured for various values of ε, the weighting scalar that penalizes control energy relative to acquisition time. That is,
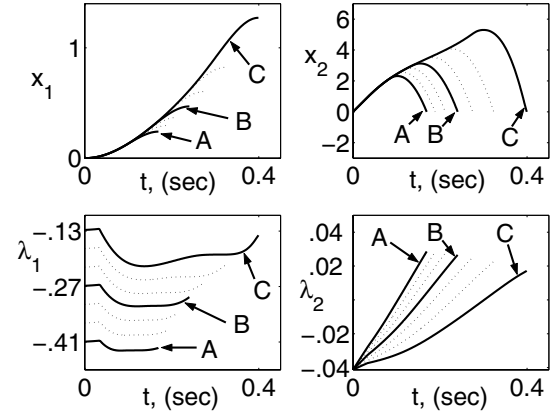
Figure 6. Continuous dependence of state and costate differential equations on initial condition $\lambda_1(0) = \lambda_{01}$ for three cases: (A) $\lambda_{01} = -0.41$, (B) $\lambda_{01} = -0.27$ and (C) $\lambda_{01} = -0.13$. In all cases, $\varepsilon = 0.01$ and the ODE integration routine is programmed to terminate once the path velocity crosses zero, i.e. $x_2 = 0$. Notice that the total distance travelled along the specified path increases monotonically with λ_{01}. This trend was observed in all investigated test cases.

the larger the ε, the greater the amount of control energy expended resulting in faster acquisition times. Likewise, the path velocity at each point along the path increases as ε is reduced. Notice that as ε is reduced to zero, the minimum-time velocity profile is reached.
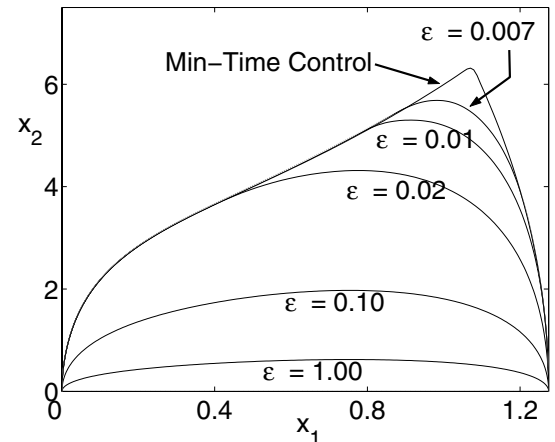
Figure 7. Time-energy optimal trajectories in the phase plane, $x_1 - x_2$, for various values of ε.

Figure (8) illustrates the time-energy optimal path acceleration trajectories, for various values of ε. Notice that the path accelerations approach zero as ε is increased. Reducing ε causes the path acceleration to increase until it reaches its upper bounds. Once this occurs the acceleration

cannot increase further, but it can remain at a maximal level over a larger part of the curve. For $\varepsilon > 0$ the path acceleration is continuous, but for $\varepsilon = 0$ the path acceleration is discontinuous.
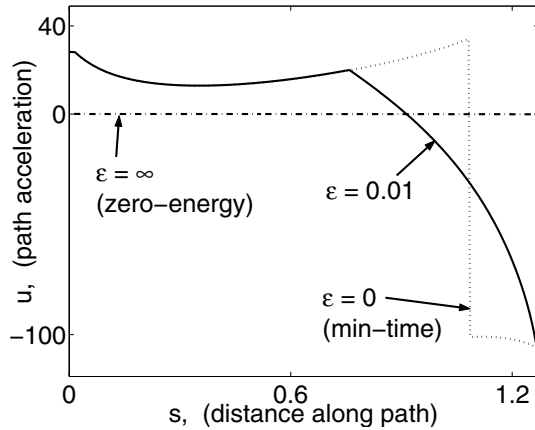
Figure 8. Time-energy optimal path acceleration trajectories, for various values of ε.

Figure (9) shows the control tendon axial force trajectories along path x_1 for each of the six control tendons at various values of ε. The tendon forces are required to satisfy $1 \leq t_i \leq 99$, for $i = 1, 2, \ldots, 6$. When the robot is moved very slowly, its tendon force trajectories approach the static-equilibrium tendon forces that correspond to the case $\varepsilon_\infty = \infty$. For this case, the tendon forces are smooth C^∞ functions of the distance along the given path. For the case that $\varepsilon_* = 0.01$, the tendon force trajectories are smooth except at two distinct corner points that correspond to points where the path acceleration constraint switches from active to inactive status. For the $\varepsilon_0 = 0$ (minimum-time control) case, the tendon force trajectories experience jump discontinuities when the path acceleration switches from its maximum to minimum value.

Figure (10) shows the control energy and motion time as a function of ε. Clearly, this plot demonstrates the trend that as the ε is increased, the acquisition time increases to infinity, but the expended control energy approaches zero. It is also interesting to observe that when ε is reduced below 0.007, the acquisition time no longer decreases even though the expended control energy continues to increase until ε is reduced below 0.001. This observation suggests that the time-energy optimal trajectory at $\varepsilon = 0.007$ is virtually just as fast as the time-optimal trajectory, but requires less control energy.

Figure (11) shows that the Hamiltonian's convexity with respect to u can be checked point-wise along specified paths. Strict convexity of the Hamiltonian with respect to control u is a sufficient condition for a local minimum of the time-energy cost function. This plot demonstrates
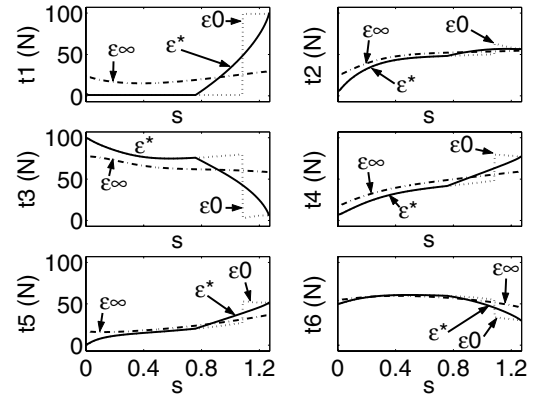
Figure 9. Control tendon axial force trajectories along path x_1 for various values of ε. Specifically, $\varepsilon_\infty = \infty$, $\varepsilon_* = 0.01$, $\varepsilon_0 = 0$. Tendon forces are required to satisfy $1 \leq t_i \leq 99$, for $i = 1, 2, \ldots, 6$.
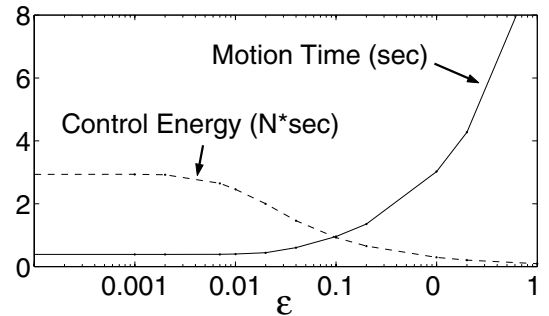
Figure 10. Control energy and motion time vs. ε. Control energy is defined here as the square root of $\int_0^T \|t - t_{stat}\|^2 d\hat{t}$ divided by the number of tendons.

that the Hamiltonian is convex at each point along the path, which implies that any infinitesimally small variation of the control trajectory $u + \delta u$ will necessarily result in an increase in the time-energy cost function.

Figure (12) shows the trajectory of the state-dependent constraint $h(x)$. This is an important plot to check, because $h(x) \leq 0$ in (17) must hold for the duration of the maneuver. If at any point along the path the constraint is violated, i.e. $h(x) > 0$, then the path acceleration is no longer feasible and at least one tendon will break or go slack. Since the constraint $h(x) \leq 0$ was not added to the Hamiltonian function with multipliers, there is no reason for this constraint to hold true. For this reason, a plot of $h(x)$ versus x_1 must be inspected to see that $h(x) \leq 0$ holds. If it does not hold, then the time-energy optimal control algorithm presented in this paper cannot offer a solution. In practice, the constraint is not violated except in cases where ε is chosen too small and the prescribed path is too curvy.
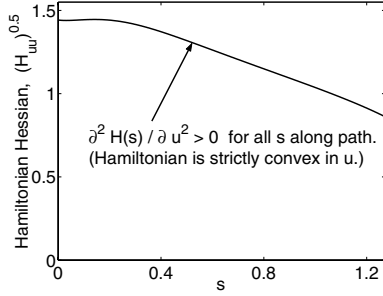
Figure 11. Strict convexity of the Hamiltonian with respect to control u can be checked point-wise along specified paths. This is a sufficient condition for a local minimum of the time-energy cost function.
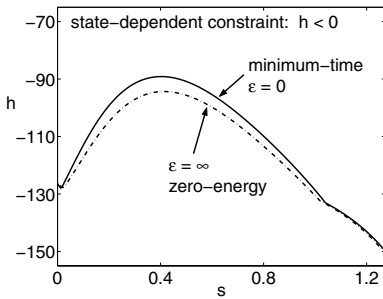
Figure 12. State-dependent constraint, $h(x) \leq 0$, must hold along the specified path as shown. This condition must be checked on a case by case basis.

5. Existence and uniqueness of solution to state/costate ordinary differential equation

Before theorem 1 can be used, its hypothesis must be satisfied. In particular, it must be shown that there exists a non-trivial solution to the system of ode's given by (27, 28, 29, 30) subject to control law (33). To facilitate the proof, substitute (33) into (30) to yield the autonomous ode's:

$$\dot{z} = F(z), \qquad z(0) = z_o \qquad (36)$$

where $z = [\, z_1 \ z_2 \ z_3 \ z_4 \,]^T = [\, \lambda_1 \ \lambda_2 \ x_1 \ x_2 \,]^T \in \mathbb{R}^4$ and $F = [\, F_1 \ F_2 \ F_3 \ F_4 \,]^T \in \mathbb{R}^4$ is defined by

$$
\begin{aligned}
F_1 &= -2\varepsilon^2 \tau^T W \left[u d_{z_3} + z_4^2 b_{z_3} \right] - \varepsilon^2 \tau^T W_{z_3} \tau - \mu^T g_{z_3} \\
F_2 &= -z_1 - 4\varepsilon^2 z_4 b^T W \tau - \mu^T g_{z_4} \\
F_3 &= z_4 \\
F_4 &= u(z)
\end{aligned}
$$

Theorem 2 *If λ_{02} is as in (35), and $\tilde{r} : [s_o, s_f] \to \mathscr{W} \subset \mathbb{R}^n$ is chosen as in (10), then for each $\lambda_{01} \in \mathbb{R}$ there exists a unique solution to the ordinary differential equations (36) on set $\mathscr{S} := \left\{ z \in \mathbb{R}^4 : s_0 \leq z_3 \leq s_f, z_4 \geq 0 \right\}$.*

Proof. To show existence and uniqueness, it suffices to show that F in (36) is piecewise Lipschitz on $\mathscr{S}$. Since $\tilde{r} \in \mathscr{W}$ for all $z \in \mathscr{S}$, then the robot's kinematics are smooth functions of its path position z_3 and velocity z_4. Since the Hamiltonian is strictly convex, then $\sigma(z)$ is smooth, and $u(z)$ is Lipschitz. Proof details for these claims are given in [1] where it is also shown that function F is a piecewise continuous function from $\mathscr{S}$ into $\mathbb{R}^4$ such that F_1 and F_2 are piecewise continuously differentiable on $\mathscr{S}$, and F_3 and F_4 are Lipschitz continuous on $\mathscr{S}$. $\diamond$

6. Conclusion

Biological systems inherently have more actuators than degrees of freedom of the mechanical motion. This allows for robustness and agility to be incorporated with minimal energy control in a way that engineers are only now beginning to understand and appreciate. In tensegrity control problems, two major obstacles present themselves: slack tendons and broken tendons. The controller in this paper prevents both. The main contribution is a control synthesis method that determines the tendon force inputs from a set of admissible (non-saturating) inputs that will move the mechanical system along a prescribed path with minimal time and energy.

References

[1] J.B. Aldrich. *Control synthesis for a class of light and agile robotic tensegrity structures*. PhD thesis, Department of Mechanical and Aerospace Engineering, University of California, San Diego, 2004.

[2] J.B. Aldrich, R.E. Skelton, and K. Kreutz-Delgado. "Control synthesis for a class of light and agile robotic tensegrity structures". In *American Control Conference*, pages 5245–5251, 2003.

[3] J.E. Bobrow, S. Dubowsky, and J.S. Gibson. "Time-optimal control of robotic manipulators along specified paths". *Int J of Robot Res*, 4(3), 1985.

[4] A.E. Bryson and Y. Ho. *Applied Optimal Control*. Taylor & Francis, 1975.

[5] Z. Shiller. "Time-energy optimal control of articulated systems with geometric path constraints". *ASME J. of Dyn Sys, Meas and Ctrl*, 118(1):139–143, 1996.

[6] R.E. Skelton, J.W. Helton, R. Adhikari, J. Pinaud, and W. Chan. "An introduction to the mechanics of tensegrity structures". In *Conference on Decision and Control*, volume 5, pages 4254–9, 2001.

[7] J.-J. E. Slotine and H. Yang. "Improving the efficiency of time-optimal path-following algorithms". *IEEE Trans Robot Automat*, 5(1):118–124, 1989.